Robust generation of superposition states

Rekishu Yamazaki,[1] Ken-ichi Kanda,[2] Fumihiko Inoue,[2] Kenji Toyoda,[1,2] and Shinji Urabe[1,2]

[1]*JST-CREST, 4-1-8 Honmachi, Kawaguchi, Saitama 331-0012, Japan*

[2]*Graduate School of Engineering Science, Osaka University, 1-3 machikaneyama, Toyonaka, Osaka 560-8531, Japan*

We describe experimental results of the generation of superposition states in a two-level system, $4s\,S_{1/2}$ and $3d\,D_{5/2}$ states, of a single calcium ion. The generation method is based on population transfer via rapid adiabatic passage (RAP), proposed by Vitanov and Shore [Phys. Rev. A **73**, 053402 (2006)]. The coherence of the generated superposition state is evaluated with a Ramsey-like interferometry method and a fringe visibility of up to 0.93 is obtained. The state generation shows strong robustness with respect to the RAP pulse parameters, including frequency chirp width and Rabi frequency.

PACS number(s): 42.50.Dv, 37.10.Ty, 03.67.−a, 42.50.Ex

I. INTRODUCTION

In the past decade, rapid technological advancement in coherent manipulation of quantum systems has generated a vast number of successful reports in the field of quantum-information processing (QIP). Ion-trap-based quantum-information processing is considered to be one of the promising candidates for a large-scale quantum computer [1]. The trapped ions in a rf pseudopotential well can have very little coupling with the external environment; thus a long coherence time of the qubit, usually prepared in ground and metastable states or hyperfine ground states, is attainable [2,3]. Fundamental elements of quantum-information processing, including qubit initialization, single- and two-qubit operation, and state readout, have already been demonstrated in the ion-trap system [4].

One of the current efforts in the ion-trap QIP has been concentrated in the development of high-fidelity and robust operations [5–8]. Two-qubit gate operations currently in use are composed of sequences of laser pulses, and the robustness of each laser pulse operation guarantees a high-fidelity gate operation as a whole. Fluctuation in the accessing laser power and frequency can alter the effective Rabi frequency of the laser pulse. Additionally, technical noise, including laser pointing instability and laser power inhomogeneity at each ion location, can alter the effective Rabi frequency, thereby diminishing the operation's fidelity. Coherent processes that are robust against these fluctuations and system instabilities could be an important part of the development of QIP. Robust state population transfer with stimulated Raman adiabatic passage (STIRAP), merely insensitive to small fluctuations in the laser power and frequency, has been well studied for a three-level system in an ensemble of atoms [9,10], and has been adopted in an ion-trap QIP experiment to yield a high population transfer fidelity of 95% [11]. A similar technique, rapid adiabatic passage (RAP) in a two-level system, performed with a frequency-chirped laser pulse, was recently used to transfer population between qubit states and a transfer fidelity of 99% was reported [12]. These studies showed robust population transfer between qubit states; however, there has not been much study reported on robust generation of superposition qubit states.

Vitanov and Shore recently showed topological equivalence between the generation of a superposition state in a two-level system and population transfer in a three-level system using the STIRAP technique [13]. We report the experimental study of the robust generation of the superposition state in a two-level system via RAP, following the description by Vitanov and Shore.

II. DESCRIPTION OF RAP FOR THE GENERATION OF SUPERPOSITION STATES

A comparison between three-level STIRAP and two-level RAP is shown in Fig. 1. In a typical three-level STIRAP [Fig. 1(a)], the amplitudes of the Raman lasers form two Gaussian-shaped pulses in a well-known "counterintuitive sequence," exciting the Raman transition to transfer population from the initial state to the target state. The overlap region of the Gaussian pulses generates the adiabatic passage between two states. For the two-level RAP [Fig. 1(b)], a single probing laser is used and the first Gaussian pulse is replaced by the detuning of the probing laser. The general idea of RAP can be described simply in a Bloch vector picture of the two-level system. The motion of the Bloch vector
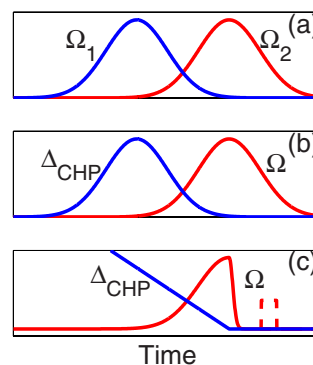
FIG. 1. (Color online) STIRAP and RAP laser parameters. (a) Three-level STIRAP: Amplitudes of each Raman laser form two Gaussian-shaped pulses in counterintuitive sequence. (b) Two-level RAP: First Gaussian pulse is replaced with laser detuning. (c) Experimental implementation of the laser parameters: The frequency chirp is modified to a linear chirp and the second half of the Gaussian amplitude pulse is turned off rapidly. A $\pi/2$ pulse (dotted line) is added for measurement of the state coherence.

R is governed by the optical Bloch equation $d\mathbf{R}/dt = \boldsymbol{\Omega} \times \mathbf{R}$, where $\boldsymbol{\Omega}$, which we denote as a torque vector, is the vector in the Bloch space representing the interaction between the light and the atom. By choosing an appropriate phase of the laser field, the torque vector can be described as

$$\boldsymbol{\Omega}(t) = \begin{bmatrix} \Omega(t) \\ 0 \\ \Delta(t) \end{bmatrix}, \qquad (1)$$

where Ω and Δ are the Rabi frequency and detuning of the probing laser in the interaction picture of the atom and laser. The polar angle of the torque vector Θ with respect to the z axis is

$$\Theta = \arctan\left(\frac{\Delta}{\Omega}\right). \qquad (2)$$

In RAP, the torque vector is initially set to orient along the Bloch vector. The adiabatic following of the Bloch vector of the motion of the torque vector is used to guide the Bloch vector direction to the preferred final state [12]. The adiabatic condition for the motion of the torque vector $\boldsymbol{\Omega}$ is given by

$$\frac{|\dot{\boldsymbol{\Omega}}|}{|\boldsymbol{\Omega}|} \ll |\boldsymbol{\Omega}|. \qquad (3)$$

The laser amplitude and the frequency can be modified to steer the torque vector direction as long as they satisfy the above condition.

It is important to mention that, for three choices of laser detuning Δ, the polar angle of the torque vector becomes independent of the Rabi frequency Ω. For $\Delta = \pm \infty$ and 0, the corresponding Θ are $\pm \pi/2$ and 0, respectively. It is this special feature that guarantees the robustness of the population transfer in Ref. [12] with RAP. For a large magnitude of Δ ($\Delta \gg \Omega$), Θ is merely independent of small drift in Ω and Δ. Similarly, in order to generate a superposition state $|\Psi\rangle = 1/\sqrt{2}(|0\rangle + e^{i\theta}|1\rangle)$, the torque vector evolution is stopped at $\Delta = 0$ and the process should be robust with respect to the variation in Ω.

III. EXPERIMENT

Detailed experimental procedures for ion trapping, cooling, and qubit state detection have been previously explained and we only discuss them briefly [14]. Relevant energy levels and transitions for the experiment are shown in Fig. 2. We trap a single $^{40}\mathrm{Ca}^+$ ion in a spherical Paul trap, with an inner radius r_0 of 0.6 mm. The secular frequency of the trap is $\omega_z = 2\pi \times 2.5$ MHz under the typical trap rf voltage and frequency, $V_{rf} = 400$ V_{pp} and $\omega_{rf} = 2\pi \times 20$ MHz, respectively. The ion is laser cooled to near the Doppler limit using the $S_{1/2} \rightarrow P_{1/2}$ transition at 397 nm. The ion is optically pumped and initialized to $S_{1/2}$, $m_j = -1/2$, identified with $|0\rangle$. The RAP pulse excites the $S_{1/2} \rightarrow D_{5/2}$ quadrupole transition at 729 nm. The frequency and polarization of the 729 nm laser is adjusted to excite the transition to the $D_{5/2}$, $m_j = -3/2$ state, identified with $|1\rangle$. After the RAP pulse, the state determina-
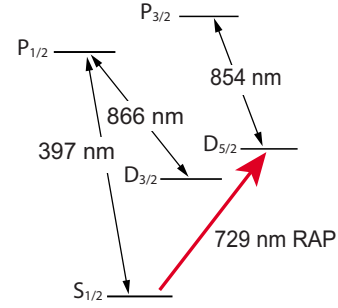
FIG. 2. (Color online) Energy level diagram of calcium ion ($^{40}\mathrm{Ca}^+$) showing the relevant transitions in the experiment. Quadrupole transition between $S_{1/2}$ and $D_{5/2}$ state is excited with a RAP pulse, wavelength of approximately 729 nm, to generate the superposition states in a single ion. Doppler cooling is performed with 397 and 866 nm lasers prior to the RAP pulse. 854 nm laser is used to repump the population excited to the $D_{5/2}$ state.

tion is performed with the shelving technique. The observation (absence) of strong uv fluorescence with a photomultiplier tube (PMT) upon turning on the cooling cycle determines the electron in the state $|0\rangle$ ($|1\rangle$). In order to generate the RAP pulse, the output of the Ti:sapphire laser is modulated with an acousto-optical modulator (AOM) in double-pass configuration. We control the amplitude and frequency of the RAP pulse with rf signal driving the AOM. The rf signal is generated with a programable direct digital synthesis (DDS) (Analog Devices, AD9858). Only a linear frequency sweep is possible with this board with a frequency update up to every 8 ns. The amplitude of the rf signal is controlled by mixing the output of the DDS signal with an output of an arbitrary wave form generator (National Instruments, PXI-7833R) based on a field-programable gate array (FPGA), generating a Gaussian laser amplitude pulse. The update rate of digital to analog output of the arbitrary wave form generator is 2 μs.

Experimental implementation of the RAP parameters is shown in Fig. 1(c). In the experiment we generate the $|\Psi\rangle = 1/\sqrt{2}(|0\rangle + e^{i\theta}|1\rangle)$ state by fixing the final detuning of the chirped frequency to be zero. First of all, the Gaussian laser frequency chirp is replaced with a linear chirp since our rf generator is only capable of linear sweeps. Second, we turn off the second half of the Gaussian laser amplitude much faster. The detuning is fixed to zero at the second half of the pulse and allows a fast turnoff without breaking the adiabatic condition. Lastly, for the evaluation of the coherence of the superposition state, a $\pi/2$ pulse is added after the RAP pulse used for the coherence determination described later. Other parameters used in the experiment include the Gaussian half-pulse width $\sigma = 12$ μs {for the Gaussian pulse shape of $\exp[-(t-t_0)^2/(2\sigma^2)]$} and $\pi/2$ pulse duration of 7.5 μs. The frequency chirp begins 72 μs before the peak of the Gaussian pulse and stops at the Gaussian peak.

The general sequence for the generation and evaluation of the superposition state is composed of five different steps. (i) The ion is Doppler cooled with the 397 and the 866 nm lasers. (ii) The state is prepared by optical pumping, where the electron is initialized to $|0\rangle$. (iii) The RAP pulse is turned on (729 nm) to excite the transition between the $|0\rangle$ and $|1\rangle$
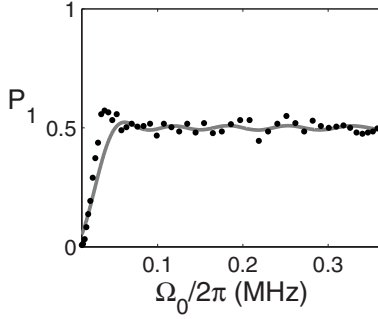
FIG. 3. Transition probability observed with various peak Rabi frequencyies Ω_0. The chirp frequency width is fixed at $\Delta_{CHP}=2\pi \times 200$ kHz. Simulation result is also shown as a solid line.

states. (iv) The state is determined by turning on the cooling cycle. (v) The second repumper laser (854 nm) is turned on to transfer the residual population in the $|1\rangle$ state back to the cooling cycle. All the beam turn-ons and turn-offs are controlled with the AOMs. We repeat this sequence 100–400 times for each RAP pulse condition. The projection measurement in step (iv) determines only the population transferred to $|1\rangle$. In order to evaluate the coherence of the superposition state, we used a method similar to Ramsey interferometry by inserting a $\pi/2$ pulse with varying phase ϕ added with respect to the phase of the RAP pulse. As in quantum state tomography in an ion-trap experiment [15], the pulse effectively rotates the basis by $\pi/2$ and enables the determination of the off-diagonal element of the state density matrix, the coherence of the state.

IV. RESULTS

We show the results of superposition state generation by the RAP pulse. For evaluation of the robustness of the superposition state generation, we measure the transfer probability to $|1\rangle$, P_1, with respect to the Rabi frequency at the Gaussian pulse peak Ω_0. We also show the results of the the measurements for the evaluation of the superposition state coherence and the relative phase between the states.

A. Evaluation of population transfer

The experimental results along with solid lines showing the simulation results obtained for the same RAP parameter are shown in Fig. 3. The data are obtained at the chirp frequency width $\Delta_{CHP}=2\pi \times 200$ kHz. The experimental results match well with the simulation and the final population is approximately 0.5 for a large range of Ω_0. Lack of population transfer can be observed for $\Omega_0 < 2\pi \times 0.05$ MHz, consistent with the simulation results. The diminished transfer probability is owing to the small Rabi frequency, which does not satisfy the adiabatic condition given in Eq. (3).

B. Ramsey method for the evaluation of coherence

We use a Ramsey-like method for the evaluation of the coherence of the generated state. As we change the phase ϕ of the $\pi/2$ pulse, we observe the well known Ramsey fringe
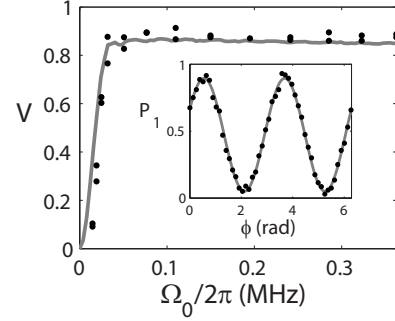
FIG. 4. Inset: Example of the observed Ramsey fringe pattern with an additional $\pi/2$ pulse after the RAP pulse along with the fitted sine curve. Visibility V is obtained from the fitted line. Main figure: visibility observed with the Ramsey-like interferometry method for various Ω_0, along with the simulation result as a solid line. The chirp frequency width is fixed at $\Delta_{CHP}=2\pi \times 200$ kHz.

pattern in the transferred population P_1. An example of the observed fringe is shown in the inset of Fig. 4. The fringe pattern is first fitted with an equation

$$P_1(\phi) = A \sin(\phi + \theta') + B, \qquad (4)$$

and the the fringe visibility $V = (P_{1max} - P_{1min})/(P_{1max} + P_{1min}) = A/B$, where P_{1max} and P_{1min} are the maximum and minimum of the transition probability, is calculated. We measure the fringe visibility with respect to various Ω_0.

The experimental results are shown in Fig. 4 along with the simulation results as solid lines. High visibility of up to 0.93 is observed and the results also show strong robustness of the coherence preservation against Ω_0. As in the case of the transfer probability, the coherence diminishes rapidly for $\Omega_0 < 2\pi \times 0.05$ MHz. The simulation results show the visibility upper limit of about 0.9 for the region of parameters that we investigated. The main cause for the loss of visibility is the laser linewidth in the simulation. Our probing laser has a linewidth of approximately 1 kHz and this value is included in the simulation. A higher visibility can be obtained by reducing the Gaussian pulse width, so that the RAP process is completed in much less than the coherence time of the laser. Our current limitation is the update rate of the arbitral wave form generator, which is 2 μs, and requires at least several tens of microseconds to generate a "smooth" RAP pulse. Despite the technical limitations, the experimental results show visibility comparable to that of the simulation and also a superb robustness against variation in Rabi frequency.

C. Evaluation of the phase variation of the superposition states

For the generation of a superposition state $|\Psi\rangle = 1/\sqrt{2}(|0\rangle + e^{i\theta}|1\rangle)$, the high fringe visibility shown in the previous section does not guarantees that the RAP process is generating the same superposition state, with the same phase factor θ, for various Ω_0. We identify variation of the phase difference θ between the qubit states from the phase of the fitted sine curve, θ'. As shown in Fig. 5, the obtained phase is approximately constant for $\Omega_0 > 2\pi \times 0.05$ MHz and obtained $\theta' = 0.17 \pm 0.22$ rad for those data, showing that the
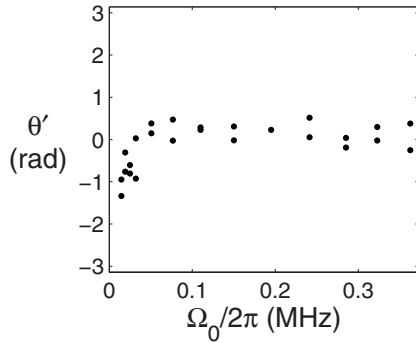
FIG. 5. Phase obtained from a sine curve fitted to the Ramsey fringe measurements for various Ω_0. For large enough Ω_0, the observed phase is approximately constant and the obtained phase is $\theta' = 0.17 \pm 0.22$ rad for the data in the region $\Omega_0 > 2\pi \times 0.05$ MHz.

RAP process is generating the superposition states of the same phase difference with the standard deviation of 0.22 rad.

D. Variation of state generation fidelity with respect to the chirp frequency width

As mentioned earlier, the RAP process should be robust as long as it satisfyies the adiabatic condition [Eq. (3)] and therefore it should show some robustness against the chirp frequency width Δ_{CHP}. As an additional test, we observe the robustness of the superposition state generation against Δ_{CHP} and the experimental results along with a simulation result in a line are shown in Fig. 6(a). The chirp frequency is updated every 50 ns in these data with Ω_0 fixed at $2\pi \times 240$ kHz. The data show a similar robustness as observed in the variation of Ω_0 and the fringe visibility is maintained to approximately 0.85 at $\Delta_{CHP} = 2\pi \times 0.5$ MHz; however, we observe quite fast deterioration of the coherence for a higher Δ_{CHP}, as shown with solid dots in Fig. 6(b). The gray dashed lines through the data points in the figure are fitted lines only to guide the eye. The origin of the fast deterioration is not well understood, but we presume that the weaker robustness at higher Δ_{CHP} may be caused by the broken adiabaticity of the RAP pulses. The digital nature of the frequency update used in the experimental results in a rapid frequency transition and the motion of the torque vector may be breaking the adiabatic condition. To confirm our presumption, we decrease the frequency update rate with the same Δ_{CHP}, which results in a larger frequency "hop" for each update, and the results are shown in the same figure as the white dots. We observed enhancement of the coherence deterioration, and the fringe visibility dropped down to 0.4 at $\Delta_{CHP} = 2\pi \times 0.3$ MHz for chirp frequency update every 1 μs.

V. DISCUSSION AND CONCLUSION

The variation in the chirp frequency width shows less robustness; however, it is more important that the process is robust against the variation in Rabi frequency. By the nature of the frequency chirp generation, controlled with rf, the chirp frequency widths do not fluctuate much in time. It
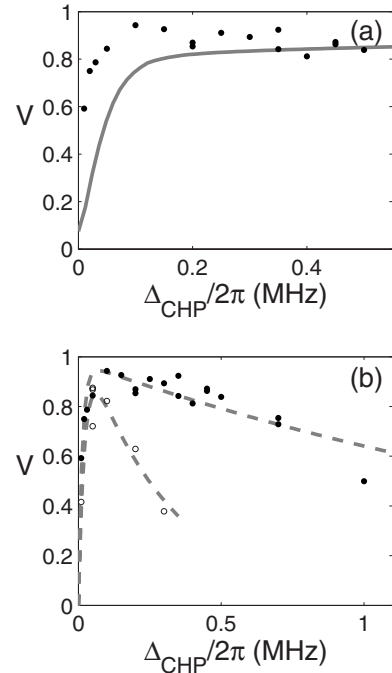
FIG. 6. Effect of the chirp frequency width variation on state generation fidelity. (a) Ramsey fringe visibility observed for various Δ_{CHP} along with a simulation result shown as a gray line. Chirp frequency update every 50 ns and $\Omega_0 = 2\pi \times 240$ kHz are used for all the data. (b) Comparison of the coherence deterioration for different frequency update rates. The data with solid dots and white dots are obtained with frequency update every 50 ns and 1 μs, respectively. The dashed lines through the data are fitted lines only to guide the eye.

helps to have a strong robustness to initially search for high-fidelity RAP parameters but it is not a critical problem. The Rabi frequency, however, can fluctuate due to many technical problems mentioned earlier. The results obtained are important in practical situations of ion-trap QIP where these noises can be some of the limiting factors. It is possible to keep the frequency chirp of the RAP pulse within the secular frequency of the trap, typically a few megahertz, so that only a carrier or one of the sideband transitions is selectively excited by the RAP. It is important that the current method of superposition state generation with RAP can be time reversed to bring the superposition state back to either qubit state. The method used by Liebfried *et al.* for the creation of a highly entangled Schrödinger cat state of multiple ions includes a collective $\pi/2$ rotation [16]. The variation of the laser intensity at ions that are spatially apart is one of the limiting factors of this method. The RAP method presented can be adopted to overcome this issue.

The state generation fidelity in this study is mainly limited by the RAP pulse duration with respect to the laser linewidth, as mentioned. Compared to a simple $\pi/2$ pulse method, the adiabatic condition of RAP requires the torque vector rotation time to be much longer than the Rabi period and the RAP method is inevitably more time consuming. The bandwidth limitation of the rf amplitude and frequency controller can also be a limiting factor for the pulse duration. In order to quantify the limit of the RAP process, we perform numeri-
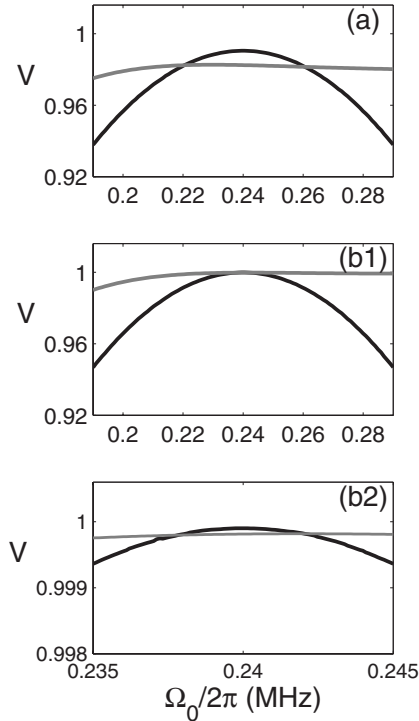
FIG. 7. Effect of the probe laser linewidth on the Ramsey fringe visibility. The simulation results for the laser linewidths of (a) 1 kHz and (b1), (b2) 10 Hz are shown with the RAP method and $\pi/2$ pulse results as gray and black lines, respectively. Comparing (a) and (b2), the $\pi/2$ pulse results show higher visibility in a much smaller region of Ω_0 for the narrower laser linewidth. A narrower laser linewidth reduces the decoherence effect of the time-consuming RAP method, and effectively increases the robustness of the RAP process.

cal simulations disregarding the technical limit on the rf control. The simulations show that the RAP pulse process can be shortened to approximately 15 μs for $\Omega_0 = 2\pi \times 240$ kHz, the typical peak Rabi frequency used in the current study. Figure 7(a) shows the simulation results of the RAP method with shortened pulse duration and the $\pi/2$ pulse method as gray and black lines, respectively, for the laser linewidth of 1 kHz. In order to compare the robustness of the $\pi/2$ pulse with that of the RAP pulse, the $\pi/2$ pulse duration is fixed at $t = (\pi/2)/(2\pi \times 240 \text{ kHz}) \simeq 1.04$ μs during the simulation. With the shorter pulse duration, the simulation result shows increased Ramsey fringe visibility of up to $V = 0.983$ for the RAP process. The visibility is much better than the current limit of $V = 0.93$ obtained from the experiment; however, the simulation with a simple $\pi/2$ pulse yielded maximum fringe visibility of $V = 0.990$. Moreover, in a wide range of Ω_0,

$0.22 < \Omega_0/(2\pi) < 0.26$ MHz, the $\pi/2$ pulse method shows higher visibility. The situation is quite different for the case of a narrow laser linewidth as shown in Fig. 7(b1), where the laser linewidth of 10 Hz is used for the simulation. Due to the long laser coherence time, the RAP process has much smaller decoherence, resulting in higher visibility for all Ω_0, while the $\pi/2$ pulse has a smaller increase in visibility. As can be seen in Fig. 7(b2), a smaller region of the same data in Fig. 7(b1), a $\pi/2$ pulse has higher visibility in a much narrower range of Ω_0, effectively increasing the robustness of the RAP process. When working with a probing laser whose coherence time is comparable to the RAP pulse duration, the decoherence introduced from the long pulse length will reduce the effective robustness with respect to the $\pi/2$ pulse. The strength of the RAP process can be enhanced in the limit of narrow laser linewidth. Our current investigation includes use of the RAP method in a Raman system, where two lasers coupling the qubit states are generated from modulation of a single laser or phase-locked via a frequency comb [17]. A physical implementation is as simple as sending one of the Raman beams through the rf-controlled AOM used in the current study. A narrow effective laser linewidth of the Raman process should substantially suppress the decoherence while retaining the benefit of the robustness of the RAP.

The fundamental limitation of this method, however, is that it requires precise knowledge to initially align the torque vector along the Bloch vector. Therefore the current method is effective for preparation or manipulation of well-known states, but its use is limited for the manipulation of an arbitrary state. With its strong robustness against the Rabi frequency, this method can be applied beyond ion-trap QIP, as in coherent manipulation of spatially large samples and of "optically thick" material, in which the laser power diminishes considerably as it propagates through the medium. This could be a key technique for the manipulation of a large ensemble of atoms such as a Bose-Einstein condensate system. It is also attractive that the technique is easily adopted experimentally. The conventional proposals for fast frequency chirp include a dynamic Stark shift with an additional laser pulse and a dynamic magnetic field shift, when states susceptible to a magnetic field are used [13]. Use of the rf manipulation is simple and also robust by its nature compared to these methods.

In conclusion, generation of superposition states with RAP is conducted with maximum interferometric fringe visibility of 0.93. The method shows strong robustness against the Rabi frequency of the probing pulse laser.

Note added. Recently, we became aware of a related work by Timoney *et al.* [18].

[1] D. Kielpinski, C. Monroe, and D. J. Wineland, Nature (London) **417**, 709 (2002).

[2] F. Schmidt-Kaler, S. Gulde, M. Riebe, T. Deuschle, A. Kreuter, G. Lancaster, C. Becher, J. Eschner, H. Häffner, and R. Blatt, J. Phys. B **36**, 623 (2003).

[3] D. J. Wineland, C. Monroe, W. M. Itano, D. Leibfried, B. King, and D. Meekof, J. Res. Natl. Inst. Stand. Technol. **103**, 259 (1998).

[4] *ARDA Quantum Information Science and Technology Roadmap*, http://qist.lanl.gov

[5] L. Aolita, K. Kim, J. Benhelm, C. F. Roos, and H. Häffner, Phys. Rev. A **76**, 040303(R) (2007).

[6] M. Riebe, K. Kim, P. Schindler, T. Monz, P. O. Schmidt, T. K. Körber, W. Hänsel, H. Häffner, C. F. Roos, and R. Blatt, Phys. Rev. Lett. **97**, 220407 (2006).

[7] P. C. Haljan, P. J. Lee, K.-A. Brickman, M. Acton, L. Deslauriers, and C. Monroe, Phys. Rev. A **72**, 062316 (2005).

[8] D. Leibfried *et al.*, Nature (London) **422**, 412 (2003).

[9] K. Bergmann, H. Theuer, and B. W. Shore, Rev. Mod. Phys. **70**, 1003 (1998).

[10] G. W. Coulston and K. Bergmann, J. Chem. Phys. **96**, 3467 (1992).

[11] J. L. Sørensen, D. Møller, T. Iversen, J. B. Thomsen, F. Jensen, P. Staanum, D. Voigt, and M. Drewsen, New J. Phys. **8**, 261 (2006).

[12] C. Wunderlich, T. Hannemann, T. Körber, H. Häffner, C. Roos, W. Hänsel, R. Blatt, and F. Schmidt-Kaler, J. Mod. Opt. **54**, 1541 (2007).

[13] N. V. Vitanov and B. W. Shore, Phys. Rev. A **73**, 053402 (2006).

[14] H. Sawamura, H. Kitamura, K. Toyoda, and S. Urabe, Appl. Phys. B: Lasers Opt. **80**, 1011 (2005).

[15] C. F. Roos, G. P. T. Lancaster, M. Riebe, H. Häffner, W. Hänsel, S. Gulde, C. Becher, J. Eschner, F. Schmidt-Kaler, and R. Blatt, Phys. Rev. Lett. **92**, 220402 (2004).

[16] D. Leibfried *et al.*, Nature (London) **438**, 639 (2005).

[17] R. Yamazaki, H. Sawamura, K. Toyoda, and S. Urabe, Phys. Rev. A **77**, 012508 (2008).

[18] N. Timoney, V. Elman, S. Glaser, C. Weiss, M. Johanning, W. Neuhauser, and C. Wunderlich, Phys. Rev. A **77**, 052334 (2008).